

## Vertical Profiles of Volcanic Aerosol and Polar Stratospheric Clouds Above Kiruna, Sweden: Winters 1993 and 1995

TERRY DESIILER<sup>1</sup> and SAMUEL J. OLTMANS<sup>2</sup>

<sup>1</sup>*Department of Atmospheric Science, University of Wyoming, Laramie, WY 82071, USA*

<sup>2</sup>*National Oceanic and Atmospheric Administration, 325 Broadway, Boulder, CO 80303, USA*

**Abstract.** Vertical profiles of aerosol were measured in February 1993, and January - March 1995 using balloon-borne particle counters released from Kiruna, Sweden. Condensation nuclei (CN) and aerosol with radii  $\geq 0.15 - 10.0 \mu\text{m}$  were measured in 8-12 size classes. The three flights in 1993 were within the polar vortex. Temperatures were below polar stratospheric cloud (PSC) threshold temperatures on one flight and a thin PSC was observed. The volcanic aerosol in the 1993 vortex was similar to that in 1992. In 1993, surface areas were  $10 - 20 \mu\text{m}^2 \text{cm}^{-3}$  and volumes  $1 - 3 \mu\text{m}^3 \text{cm}^{-3}$ . In 1995 three of five flights were within the polar vortex. The volcanic aerosol had decreased to  $3 - 7 \mu\text{m}^2 \text{cm}^{-3}$  and  $0.1 - 0.4 \mu\text{m}^3 \text{cm}^{-3}$ . The top of the volcanic aerosol layer in both years was near 500 K potential temperature ( $\sim 20 \text{ km}$ ). A thick nitric acid and water PSC was observed in January 1995. In the thickest region of this PSC nearly all CN were observed to be activated, and surface areas of  $5 - 10 \mu\text{m}^2 \text{cm}^{-3}$  were calculated. The volumes observed in this PSC were closer to what would be expected for particles composed of nitric acid trihydrate than for ternary solution droplets. In 1993 the opposite was observed, the volumes in the thin PSC were closer to what would be expected for ternary solution droplets.

**Key Words:** Polar stratospheric clouds, stratospheric aerosol, water vapor profiles, decay of Pinatubo aerosol.

### 1. Introduction

Studies of the aerosol content of the polar stratosphere have followed the renewed interest in the polar stratosphere sparked by the first evidence of significant ozone depletion there [Farman et al., 1985]. Aerosol particles, particularly PSC particles, provide sites for heterogeneous chemical reactions which free reactive chlorine from its reservoir species and remove reactive nitrogen from the polar stratosphere [see e.g. Solomon, 1990]. Crutzen and Arnold [1986] and Toon et al. [1986] first suggested that nitric acid and water were the main constituents of particles within stratospheric clouds observed to form at temperatures above the frost point. Laboratory measurements then identified nitric acid trihydrate (NAT) as a thermodynamically stable phase for non-ice PSC particles at stratospheric temperatures and pressures [Hanson and Mauersberger, 1988]. In the Antarctic, field measurements demonstrated that  $\text{NO}_y$  is incorporated into PSC particles, and that cloud boundaries generally coincide with temperatures where

the saturation with respect to NAT is greater than 1.0 [Fahey et al., 1989; Poeschel et al., 1989]. More recent Antarctic measurements, however, demonstrate that such a clear correspondence is not always the case [Dye et al., 1996]. In the Arctic, the correspondence between PSC cloud boundaries and saturation with respect to NAT has not been easy to interpret. Measurements there often indicate an absence of PSCs in air that is supersaturated with respect to NAT, and significant PSC growth only at quite high supersaturations with respect to NAT [Rosen et al., 1989; Hofmann et al., 1990; Schlager et al., 1990; Dye et al., 1992; Kawa et al., 1992]. These observations of discrepancies between PSC occurrence and the phase boundaries for NAT has led to speculation that PSC particles may be composed of hydrates of  $\text{HNO}_3$  other than NAT [Arnold, 1992], to additional work investigating the growth of sulfuric acid aerosol due to the uptake of  $\text{HNO}_3$  and  $\text{H}_2\text{O}$  [Worsnop et al., 1993; Zhang et al., 1993; Molina et al., 1993], and to new models of PSC particle growth involving condensation of  $\text{HNO}_3$  into liquid solution droplets [Tabazadeh et al., 1994; Drdla et al., 1994; Carslaw et al., 1994]. Most of the new models and some lab results [Marti and Mauersberger, 1993] suggest that the water to  $\text{HNO}_3$  molar ratio in many PSCs is significantly greater than the 3:1 of NAT.

During the winters of 1993 and 1995 aerosol concentrations in the north polar vortex were measured using optical particle counters released on balloons from ESRANGE (68°N, 21°E) near Kiruna, Sweden. In 1993 three measurements were completed within the polar vortex during February. Volcanic aerosol, from the eruption of Mt. Pinatubo in June 1991, dominated the aerosol measurements on these three flights, and little change in the volcanic aerosol was observed between the winters of 1992 and 1993. The 1995 measurements were in conjunction with the 1995 Second European Stratospheric Arctic and Mid latitude Experiment balloon campaign at ESRANGE. Aerosol particle counters were included on five flights. Three of these flights were completed within the polar vortex (21, 28 January and 20 March), one was completed on the edge of the vortex (3 February), while one was completed outside of the vortex (2 March). Polar stratospheric clouds (PSCs) were detected on 21 January 1995, and on 10 February 1993. This paper presents the results of these measurements.

The aerosol instruments used measure the number concentration of condensation nuclei (CN) ( $r > 0.01 \mu\text{m}$ ) and optically detectable aerosol ( $r \geq 0.15 \mu\text{m}$ ). The optical aerosol counters, following an original design by Rosen [1964], count and size aerosol particles drawn into a scattering region. The size is determined from measurements of the intensity of the scattered light at 40 degrees from the forward direction, using Mie theory and assuming spherical particles with an index of refraction of 1.45 [Hofmann and Deshler, 1991]. Nominally particles in the size range 0.15 to 10.0  $\mu\text{m}$  radius are measured in either 8 or 12 size classes. For applications involving the measurement of aged volcanic aerosol, the size range is reduced to 0.15 - 2.0  $\mu\text{m}$ . For CN, the particles are forced to grow to an optically detectable size with a growth chamber using ethylene glycol vapor. The minimum detectable concentration for aerosol  $\geq 0.15 \mu\text{m}$  is approximately  $0.0006 \text{ cm}^{-3}$ . The uncertainty of the measurement depends on the number of particles counted. For aerosol  $\geq 0.15 \mu\text{m}$  radius the uncertainties for concentrations of 0.001 to  $1.0 \text{ cm}^{-3}$  are 75 to 2%. For CN the uncertainties for concentrations of 1.0 to  $10.0 \text{ cm}^{-3}$  are 8 to 3%.

## 2. Observations and Discussion

Figure 1 displays vertical profiles of aerosol mixing ratio, temperature, and water vapor as a function of potential temperature for: 1a) two aerosol measurements in 1993, 1c) - 1d) five aerosol measurements in 1995, and 1b) water vapor measurements in 1993 and 1995. The cumulative concentrations shown are for CN and for particles with radius  $\geq 0.15$ ,  $0.5$ , and  $1.0 \mu\text{m}$ . Air temperatures corresponding to the aerosol measurements (center panels Figure 1) are compared to equilibrium existence temperatures for ice, liquid ternary aerosol (LTA), and NAT, assuming 5 ppmv water vapor and 5 ppbv  $\text{HNO}_3$ . The LTA temperatures were selected, somewhat arbitrarily, as the temperature where significant volume change begins to occur during the growth of LTA. LTA volumes as a function of pressure and temperature were calculated using the analytic model of Carslaw et al., [1994].

During 8 - 10 February 1993 at both 475 and 550 K the polar vortex was displaced towards Scandinavia, elongated along the dateline meridian, and roughly symmetrical about the Greenwich meridian. Between 8 and 10 February the coldest air moved east, along  $70^\circ\text{N}$ , from just east of Greenland to just west of Scandinavia, and the polar vortex, defined by potential vorticity analysis, moved  $2 - 3^\circ$  to the south along the Greenwich meridian. On both days the inside edge of the southern boundary of the polar vortex was over Kiruna, with Kiruna slightly further inside the vortex by 10 February. The tropopause was near 310 K (10 - 11 km) on both days.

The two 1993 profiles display similar mixing ratios below about 380 K, Figure 1a). On 10 February at 330 K the top of a cirrus cloud, which was 3 km thick, is evidenced by the increased concentration of  $r \geq 1.0 \mu\text{m}$  particles. On 10 February the temperature is below the NAT point from 370 - 480 K, and falls below the LTA temperature from 380 to 410 K and from 425 - 460 K. At the lower point there is a slight enhancement in the mixing ratio for particles  $\geq 0.5$  and  $1.0 \mu\text{m}$ , but not for particles  $\geq 0.15 \mu\text{m}$ . Between 425 and 460 K there is an enhancement by a factor of 2 - 3 in the mixing ratio for aerosol  $\leq 0.5 \mu\text{m}$ , and some particles  $\geq 1.0 \mu\text{m}$  are observed at the lower boundary of this region. Temperatures between 425 and 460 K are slightly colder than between 380 and 410 K, but the supercooling with respect to NAT or LTA remains about the same. Above 470 K, the mixing ratio of  $0.15 \mu\text{m}$  particles on 10 February decreases below the measurement on 8 February. This could reflect the fact that the vortex was slightly further over Kiruna on 10 February as mentioned above; however, a later profile on 18 February which was taken when the vortex was more closely centered over Kiruna displayed a profile similar to that of 8 February.

The measurements in 1995 are shown in Figures 1c) - 1d). The aerosol profiles in Figure 1c) were all taken within the polar vortex. The profiles in Figure 1d) were taken on the edge of the vortex (3 February) and outside of the vortex (2 March). The temperatures on these two flights are not shown since they were both warmer than 205 K throughout the stratosphere. The aerosol mixing ratio profiles for the cases when the temperature is greater than the NAT equilibrium temperature are all quite similar, except for 2 March above 420 K, when the air was from the mid latitudes. The slight differences in aerosol mixing ratio, 28 January to 20 March, disappear if the 28 January profile is displaced downward 20 K (1 km) in altitude. This implied descent rate, 0.02

$\text{cm s}^{-1}$ , is at the low end of the diabatic descent rates calculated by Schoeberl et al. [1992] for the Arctic vortex.

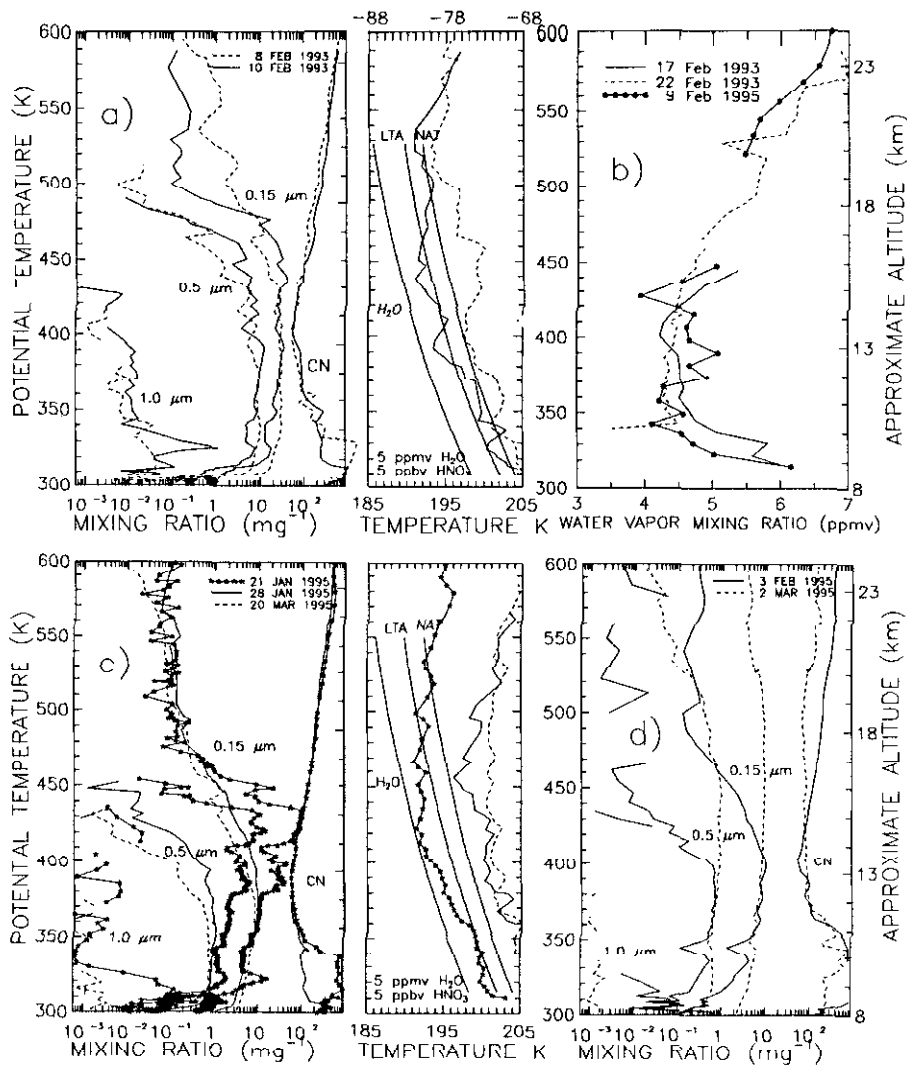


**Figure 1.** a) Aerosol and temperature measurements completed on 8 and 10 February 1993. b) Water vapor mixing ratios measured on 17 and 22 February 1993 and 9 February 1995. c) Aerosol and temperature measurements completed in 1995 within the polar vortex (21 and 28 January, 20 March). d) Aerosol measurements completed in 1995 on the edge of the vortex (3 February) and outside of the vortex (2 March). The temperatures for the two flights shown in d) were warmer than 205 K throughout the stratosphere and are not shown. Aerosol profiles for CN and for particles with radius  $\geq 0.15, 0.5, 1.0 \mu\text{m}$  are shown. The air temperature is compared to equilibrium temperatures for nitric acid trihydrate [Hanson and Mauersberger, 1988] and water ice assuming 5 ppmv  $\text{H}_2\text{O}$  and 5 ppbv  $\text{HNO}_3$ . Using the same vapor concentrations, the temperature for the initiation of liquid ternary aerosol was estimated using the analytic model of Carslaw et al. [1994]. There were problems with the water vapor measurements between 450 and 520 K on 9 February 1995, and above 450 K on 17 February 1993.

Meteorological analyses indicated that from 21–22 January 1995 the polar vortex was elongated with an axis extending from the North Atlantic to Eastern Siberia. Based on trajectory analysis, air above 380 K was confined within the polar vortex for at least the previous week. Potential vorticities (PV) over Kiruna and at the vortex edge for all flights in 1995 are given in Table 1. Even though the PV at 380 K is close to the value at the vortex boundary on 21 and 28 January, the vortex edge defined by a tight PV gradient was approximately 900 (600) km from Kiruna on 21 (28) January. On 3 February trajectories below 475 K had origins in the mid latitudes, while between 475 and 600 K the edge of the polar vortex was above Kiruna. On 2 March Kiruna was outside of the polar vortex throughout the stratosphere. On 20 March the air passing over Kiruna at all levels above 350 K had for at least the past 10 days been confined within the polar vortex.

Table 1. Potential vorticity (in units of  $10^{-6} \text{ km}^2 \text{ kg}^{-1} \text{ s}^{-1}$ ) over Kiruna compared with that at the vortex edge nearest to Kiruna for potential temperature surfaces of 380, 435, and 475 K. The value of PV at the center of the region of maximum PV gradient is used to define the vortex boundary.

Date	Kiruna (Vortex Edge)	Kiruna (Vortex Edge)	Kiruna (Vortex Edge)
Potential Temp.	380 K	435 K	475 K
21 Jan. 1995	12 (11)	34 (22)	54 (42)
28 Jan. 1995	14 (12)	35 (26)	55 (40)
3 Feb. 1995	11 (11)	33 (24)	50 (40)
2 Mar. 1995	9.5 (11)	15 (26)	22 (40)
20 Mar. 1995	16 (12)	30 (22)	48 (42)

Comparing the relatively consistent mixing ratio profiles for the volcanic aerosol from year to year, a factor of 4 to 5 decrease in aerosol mixing ratio is observed between 1993 and 1995 for aerosol particles  $\leq 0.5 \mu\text{m}$ . In addition there are almost no aerosol particles as large as  $1.0 \mu\text{m}$  left in the stratosphere by 1995. A similar change is not observed for the CN concentrations. Comparing the CN mixing ratios in all profiles, except for 2 March 1995, suggests that CN concentrations are stable from year to year and are insensitive to position within the vortex or time of year. The one unusual profile, 2 March, was observed outside of the polar vortex. For CN in the stratosphere the coagulation rate is very slow for concentrations  $< 10 \text{ cm}^{-3}$  and gravitational effects are negligible. The primary removal mechanisms are at the base of the stratosphere where the profiles on these soundings do display some structure.

The other notable features in Figure 1 appear on the 21 January 1995 profile, Figure 1c). The large mixing ratios for particles  $\geq 1.0 \mu\text{m}$  below 330 K are associated with a 6 km thick cirrus cloud layer which extended  $\sim 10 - 20 \text{ K}$  above the tropopause. The increased aerosol mixing ratios between 380 and 460 K are evidence of a striking PSC. PSC condensation can also be observed between 340 and 380 K for  $0.5 - 1.0 \mu\text{m}$  particles on 21 January 1995, and for the altitude range 430 - 470 K on 10 February 1993. The PSC on 10 February is much less evident than the one on 21 January 1995; however, considering the temperature, and the stability of the volcanic aerosol, it is still thought that some water and nitric acid have condensed in the 1993 case.

One of the most notable features of the PSC on 21 January 1995 is the convergence of the concentration of particles  $\geq 0.15 \mu\text{m}$  with that of CN between 410 and 440 K, indicating that nearly all particles available for condensation took part in the growth of

PSC particles within this cloud. This occurs at the coldest temperature in the profile. In the Arctic the complete activation of all CN within a PSC has been observed before. Hofmann et al. [1990] observed over 90% of CN becoming active within a PSC in January 1990. Dye et al. [1990] observed an unusual case where the concentration of particles within a PSC appeared to be greater than the CN concentration outside of the PSC. In the Antarctic there has been only one case when more than 50% of the CN population was observed to participate in PSC condensation [Deshler et al., 1991]. Thus this feature seems to be more characteristic of Arctic PSCs, at least during the periods when PSCs in both regions have been measured.

Water vapor measurements were completed at Esrange on 17 and 22 February 1993 and 9 February 1995 using a small frost point hygrometer [Vömel et al., 1995]. The water vapor mixing ratio profiles from these three flights, shown in Figure 1b), are quite similar, particularly comparing 22 February 1993 and 9 February 1995. These measurements are also similar to Arctic measurements in the winter of 1991/1992 [Ovarlez and Ovarlez, 1994]. Below 470 K, in the region of PSCs, all three soundings are consistent in showing 4 - 5 ppmv of water vapor within the polar vortex.

The assumption of an  $\text{HNO}_3$  mixing ratio profile for calculating NAT equilibrium and LTA initiation temperatures is based on MIPAS and CEASAR measurements which indicated 5 - 7 ppbv  $\text{HNO}_3$  mixing ratio between 370 and 470 K on 11 February 1995 [H. Oelhaf, personal communication, and F. Murcray, personal communication]. Measurements from the microwave limb sounder (MLS) on the UARS satellite [Santee et al., 1996] near Kiruna on 9 February 1993 indicate 4 - 5 ppbv  $\text{HNO}_3$  in this same altitude region. MLS measurements for January 1995 are not yet available. Measurements over Kiruna in the winter of 1991/1992 indicate that  $\text{HNO}_3$  increases from about 3 to about 8 ppbv in the altitude range 370 - 470 K [Oelhaf et al., 1994; Spreng and Arnold, 1994; Murcray et al., 1994]. Thus 5 ppbv  $\text{HNO}_3$  in this altitude regions seems reasonable, while 10 ppbv is at the upper limit of the observations.

On 21 January 1995 the temperature at 430 K just reaches the condensation point for ice for 5 ppmv  $\text{H}_2\text{O}$ . The fact that water vapor in this altitude range was 4.5 ppmv on 9 February 1995, that there are no sudden changes in particle mixing ratio confined to the region where the temperature is close to the frost point, and that the mass mixing ratios calculated from the size distributions are much below that expected for water all suggest that this is not an ice cloud.

Aerosol volumes and surface areas are calculated from the aerosol measurements using either unimodal or bimodal lognormal size distributions which give cumulative concentrations close to those measured [Hofmann and Deshler, 1991; Deshler, 1994]. Each lognormal distribution is specified by three parameters, the total number concentration,  $N_i$ , the median radius,  $r_i$ , and the distribution width,  $\sigma_i$ . The impact of measurement uncertainty, due to counting statistics, on the lognormal parameters and the derived surface area and volume has been estimated using a Monte Carlo simulation. Average variations of 10 to 20%, with a maximum variation of 60%, were found for surface area and volume concentrations and for  $\sigma_1$ ,  $r_2$ , and  $\sigma_2$  [Deshler et al., 1993]. Variations in  $r_1$  and  $N_2$  were as high as a factor of two for small values of these quantities.  $N_1$  is measured with the CN counter and has an uncertainty of < 3% for concentrations of  $10 \text{ cm}^{-3}$ .

Uncertainties associated with using an index of refraction of 1.45 to estimate particle size can lead to a systematic error dependent on the true refractive indices of the particles sampled. Changes in particle index of refraction between 1.37 and 1.51 can cause changes of up to 8% in estimated particle radius. To estimate the errors associated with particle indices of refraction differing from 1.45, size distributions were refit to the concentration measurements for a range of indices of refraction. Neglecting PSCs, the index of refraction of sulfuric acid aerosol, for water vapor mixing ratios of 5 ppmv, are anticipated to be 1.41 - 1.45 for the range of stratospheric temperatures [Steele and Hamill, 1981]. Variations of particle index of refraction in this range can cause underestimates of surface areas and volumes by an average of 5% with a standard deviation of 10%. Variations are larger for measurements involving PSCs. For the 21 January 1995 data between 370 and 500 K, surface area and volume estimates were made for particles with indices of refraction in the range 1.37 - 1.51. For surface area the result was an underestimate by an average of 2%, standard deviation 20%, while for volume the underestimate averaged 10%, standard deviation 60%. Combining the uncertainties associated with counting statistics, which affects measurement precision, with the uncertainties associated with variations of index of refraction, which affects measurement accuracy, an overall uncertainty of  $\pm 30\%$  is used for the volume and surface area estimates.

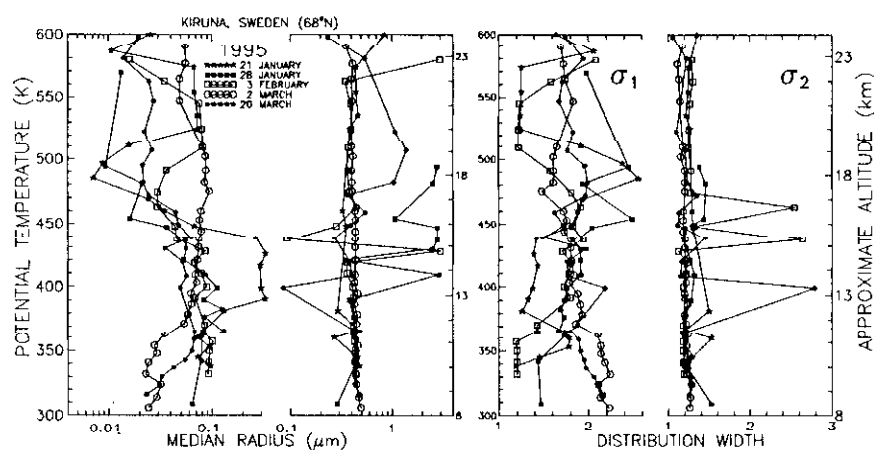
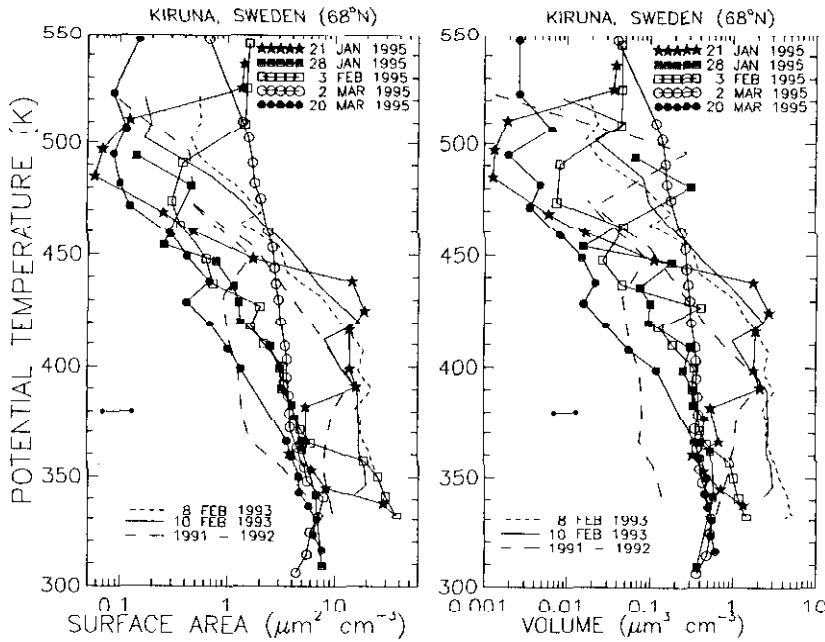


Figure 2. Vertical profiles of the median radii (two left hand panels) and distribution widths (two right hand panels) used for the unimodal and bimodal lognormal fits to the aerosol counter measurements completed in 1995.

Size distributions were fitted to 0.5-km averages of the data between the tropopause and the top of the aerosol layer for each flight. An indication of the variation of the parameters used for these lognormal fits is presented in Figure 2. The median radii and distribution widths for the first and second modes of the lognormal distributions obtained are presented as a function of altitude for the 5 flights in 1995. Since some of the measurements were fit with unimodal distributions every point in the first mode does not necessarily have corresponding points in the second mode. For example, the PSC on 21 January between 380 and 460 K was adequately represented with a

unimodal distribution. The unimodal median radius for this PSC was  $0.3 \mu\text{m}$ , about a factor of 4-5 above the volcanic aerosol small mode median radius. The PSC distribution was also quite narrow, width 1.1 -1.2. Such a narrow unimodal distribution might be expected for condensational growth of all particle sizes as indicated by the complete activation of all CN. The volcanic aerosol within the vortex in 1995 is still primarily bimodal, although the large particle lognormal distributions are quite narrow and the median radii are relatively constant at about  $0.5 \mu\text{m}$ . There are exceptions to this pattern, notably on 28 January. As might be expected the small particle mode of the volcanic aerosol size distribution shows little variation between measurements inside the vortex and outside, except at the base of the stratosphere and above 450 K, where very little volcanic aerosol resides within the vortex due to the polar night subsidence.



**Figure 3.** Aerosol surface area and volume concentrations estimated from size distributions fitted to the aerosol measurements completed in 1993 and 1995. For reference the surface areas and volumes measured in 1992 and 1991 from Esrange are included (lines with long dashes). The two error bars shown reflect an uncertainty of  $\pm 30\%$  in the surface area and volume estimates.

Based on the unimodal/bimodal size distributions fit to the measured cumulative concentrations, surface area and volume concentrations were calculated. Vertical profiles of surface area and volume are shown in Figure 3. The 1993 measurements, a typical measurement of the volcanic aerosol within the polar vortex in 1992, and a pre-Pinatubo measurement are also included. From 1992 to 1993 there was relatively little change of the volcanic aerosol profiles in the polar vortex. By 1995, however, there has



been about a factor of 5 decrease in surface area density and a factor 10 decrease in volume over the intervening two years. This reflects similar decreases observed in the mid latitudes [Jäger et al., 1995; Thomason et al., 1997]. Comparing these results to a measurement from Kiruna in 1991, prior to the eruption of Pinatubo, indicates that pre-Pinatubo levels may be reached by the winter of 1996.

Within the PSC observed on 21 January 1995 the surface areas increase to 15 - 20  $\mu\text{m}^2 \text{cm}^{-3}$  and the aerosol volume to 2 - 3  $\mu\text{m}^3 \text{cm}^{-3}$ . These are larger by factors of 5 - 10 for both surface area and volume than the measurements within the volcanic aerosol in both January and March 1995. The surface areas and volumes within this PSC are similar to measurements within the Arctic Pinatubo cloud in 1992 and in 1993.

To further investigate the characteristics of the two PSCs observed, one in 1993 and one in 1995, the volumes in Figure 3 were compared to expected volumes for two types of PSC particles, NAT and LTA. The Carslaw et al. [1994] analytic model was used to predict the LTA and NAT volumes at each pressure and temperature level for the two profiles, 10 February 1993 and 21 January 1995. For each profile the calculations were initialized with an  $\text{H}_2\text{SO}_4$  volume mixing ratio profile obtained from the aerosol volumes measured on 8 February 1993 and 28 January 1995. The calculations were repeated for the range of nitric acid and water vapor concentrations expected, 4 ppmv  $\text{H}_2\text{O}$ , 5 ppbv  $\text{HNO}_3$ , to 5 ppmv  $\text{H}_2\text{O}$ , 10 ppbv  $\text{HNO}_3$ . The results of the calculations along with the aerosol measurements are shown in Figure 4.

For 10 February 1993 the increase in aerosol mixing ratios, 380 - 410 K, for particles  $\geq 0.5 \mu\text{m}$  did not contribute significantly to either the aerosol surface area (not shown) or volume. From 425 - 460 K there is a slight increase in both aerosol surface area and volume, but not above the boundaries of the errors of the 8 and 10 February 1993 measurement. Particle volumes on 10 February are well within the range expected for LTA, and below that expected for NAT.

In 1995, when the stratospheric aerosol have been considerably reduced, the increases in aerosol surface area and volume are clearly evident in the PSC observed on 21 January 1995. In this case the volume observed within the PSC falls within the range predicted for NAT, but can be explained using the LTA model only if we assume 5 ppmv  $\text{H}_2\text{O}$  and 10 ppbv  $\text{HNO}_3$ . Based on previous  $\text{HNO}_3$  measurements in the Arctic in 1992 [Oelhaf et al., 1994; Spreng and Arnold, 1994; Murcray, 1994], MLS measurements in February 1993 [Santee et al., 1996], and the MIPAS measurements in February 1995 [H. Oelhaf, personal communication] the  $\text{HNO}_3$  mixing ratio at the altitude of the PSC in 1995 is not thought to be as high as 10 ppbv. Thus the suggestion is that this PSC was composed primarily of NAT particles.

A PSC measurement which closely parallels the one in January 1995 was made at Kiruna in January 1990 [Hofmann et al., 1990]. In that case, below the main PSC layer, particles  $\geq 0.5 \mu\text{m}$  took part in the condensation process at supersaturations with respect to NAT of about 1.0. Above this, the main PSC layer occurred at temperatures 3 - 5 K below the NAT equilibrium temperature. Over 90% of the CN grew to sizes  $\geq 0.15 \mu\text{m}$ . Very few particles as large as  $1.0 \mu\text{m}$  were observed. The condensed phase  $\text{HNO}_3$ , assuming a NAT aerosol, was 2 - 4 ppbv in this case, which is consistent with the  $\text{HNO}_3$  profile measured at that time. The size distributions within the main PSC layer in 1990 were also found to be unimodal with median radii of  $0.2 \mu\text{m}$  and distribution widths  $< 1.5$ . Differences between the 1990 and 1995 PSCs occur in the value of the

median radii, distribution widths, altitude, and cooling rate. The PSC in 1995 had larger median radii ( $0.3 \mu\text{m}$ ) and narrower size distributions, occurred at a lower altitude, and was associated with larger cooling rates. In 1990 based on trajectory analysis at the altitude of the PSC, the NAT threshold temperature, 193 K, was crossed 20 hours and 2000 km upstream of Kiruna. The cooling rate from that point to Kiruna was estimated to be  $6 \text{ K day}^{-1}$  [Schlager et al., 1990]. In 1995 trajectories were similar at all altitudes between 350 and 490 K. In the previous 12 hours, the air moved northward from the southern regions of the United Kingdom to Kiruna while cooling. At 430 K the NAT temperature, 197 K, was crossed 12 hours and 1400 km south of Kiruna. The cooling from that point to Kiruna was estimated to be  $10 \text{ K day}^{-1}$  in the thickest region of the PSC and in the thinner PSC below. A slower cooling rate and longer growth times for the 1990 case would be consistent with a broader size distribution and a smaller median radii. During the slower growth in 1990 the larger particles may consume more of the vapor, reducing the growth of smaller particles.

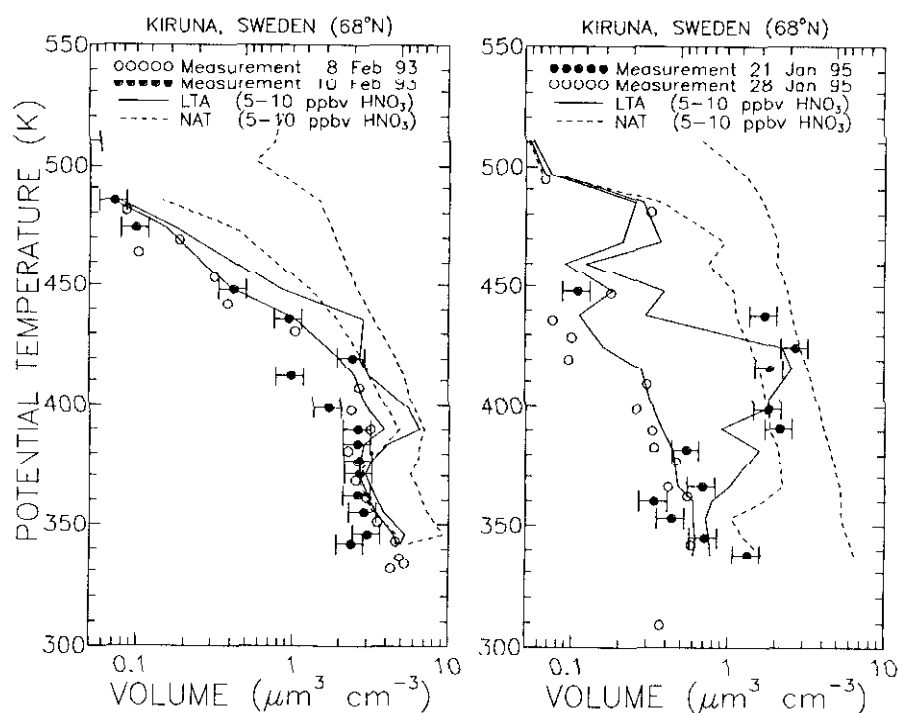


**Figure 4.** Left panel, vertical profiles of aerosol volume on 8 (open circles) and 10 (closed circles with error bars) February 1993. Right panel, aerosol volume on 21 (closed circles with error bars) and 28 (open circles) January 1995. In both panels a range of theoretical aerosol volumes for NAT and LTA are calculated assuming 4 ppmv  $\text{H}_2\text{O}$ , 5 ppbv  $\text{HNO}_3$  and 5 ppmv  $\text{H}_2\text{SO}_4$ , 10 ppbv  $\text{HNO}_3$ . For the calculated volumes the sulfuric acid mixing ratio profile is inferred from the measured aerosol volumes for the non-PSC case in each year, 8 February 1993 and 28 January 1995.

### 3. Summary and Conclusion

Aerosol profiles for particles ranging in size from CN to 10.0  $\mu\text{m}$  radius were measured in the Arctic near Kiruna, Sweden, using balloon-borne aerosol counters. Measurements were completed on 5 days in 1995, January - March. Three of these measurements were conducted within the polar vortex while one was on the edge of the vortex and one was outside the vortex. A thick PSC was observed at temperatures of 193 - 195 K between potential temperatures of 400 and 460 K on 21 January 1995. For the rest only volcanic aerosol were observed. Within the vortex the top of the volcanic aerosol was located at about 500 K (20 km), while outside the vortex the aerosol extended to near 700 K, 30 km.

Measurements were also completed on 3 days in February 1993. All three of these measurements were within the polar vortex. A thin PSC was observed on one flight, 10 February 1993, at temperatures of 192 K. The top of the volcanic aerosol profile was also near 500 K in 1993. Water vapor profiles using a frost point hygrometer in both 1993 and 1995 indicated a water vapor content of 4 -5 ppmv for the Arctic polar vortex between 330 and 480 K.

The aerosol measurements were used to estimate aerosol surface area and volume densities by fitting either unimodal or bimodal lognormal distributions to the concentration measurements. For the volcanic aerosol measurements, measurements which were too warm for PSCs, almost no change was observed between the winters of 1992 and 1993; however, by 1995 the volcanic aerosol surface area densities were observed to be reduced from 10 - 20  $\mu\text{m}^2 \text{cm}^{-3}$  in 1992 and 1993 to 3 - 7  $\mu\text{m}^2 \text{cm}^{-3}$  by 1995.

In the PSC observed in 1995 over 90% of the CN took part in the condensation process and the concentrations of particles between 0.5 and 0.15  $\mu\text{m}$  were increased by factors of 10 - 20 over the sulfuric acid aerosol. Surface areas within the PSC in 1995 increased to 15 - 20  $\mu\text{m}^2 \text{cm}^{-3}$ . A similar large increase in PSC surface areas was not observed in 1993; however, the supercooling with respect to the thermodynamically stable phases of  $\text{HNO}_3$  and  $\text{H}_2\text{O}$  was greater in 1995 than in 1993. Aerosol volumes for the two observed PSCs were compared with theoretical estimates of aerosol volume for NAT and LTA, assuming vapor mixing ratios of 4 ppmv  $\text{H}_2\text{O}$ , 5 ppbv  $\text{HNO}_3$ , and 5 ppmv  $\text{H}_2\text{O}$ , 10 ppbv  $\text{HNO}_3$ . These comparisons indicate that in 1993 the observed PSC volumes were too small to be consistent with NAT, but were consistent with LTA. In 1995 the observed PSC volumes were within the range predicted for NAT and consistent with LTA only for  $\text{HNO}_3$  mixing ratios of 10 ppbv. Based on previous measurements, an  $\text{HNO}_3$  mixing ratio of 10 ppbv seems high for this altitude region, suggesting this Arctic PSC was composed primarily of NAT.

### Acknowledgments

Gratitude is extended to L. Womack, D. Fitzgerald, B. Johnson, and W. Rozier for instrument preparations and for work in the field. We also thank R. MacKenzie and another anonymous reviewer for helpful comments on the manuscript. This work was conducted under the auspices of SESAME and financed partly by the EC and partly by the US National Science Foundation.

## References

- Arnold, F. (1992) Stratospheric aerosol increases and ozone destruction: Implications from mass spectrometer measurements, *Ber. Bunsenges Phys. Chem.*, **96**, 339-350.
- Carslaw, K. S., B. P. Luo, S. L. Clegg, Th. Peter, P. Brimblecombe, and P. J. Crutzen (1994) Stratospheric aerosol growth and HNO<sub>3</sub> and water uptake by liquid particles *Geophys. Res. Lett.*, **21**, 2479-2482.
- Crutzen P. J. and F. Arnold (1986) Nitric acid cloud formation in the cold Antarctic stratosphere: a major cause for the springtime ozone hole, *Nature*, **324**, 651-654.
- Deshler, T., A. Adriani, D. J. Hofmann, and G. P. Gobbi (1991) Evidence for denitrification in the 1990 Antarctic spring stratosphere: II Lidar and aerosol measurements, *Geophys. Res. Lett.*, **18**, 1999-2002.
- Deshler, T., B. J. Johnson, and W. R. Rozier (1993) Balloonborne measurements of Pinatubo aerosol during 1991 and 1992 at 41°N, vertical profiles, size distribution, and volatility, *Geophys. Res. Lett.*, **20**, 1435-1438.
- Deshler, T. (1994) In Situ measurements of Pinatubo aerosol over Kiruna on four days between 18 January and 13 February 1992, *Geophys. Res. Lett.*, **21**, 1323-1326.
- Drdla, A., A. Tabazadeh, R. P. Turco, M. Z. Jacobsen, J. E. Dye, C. Twohy, and D. Baumgardner (1994) Analysis of the physical state of one Arctic polar stratospheric cloud based on observations, *Geophys. Res. Lett.*, **21**, 2475-2478.
- Dye, J. E., et al. (1990) Observed particle evolution in the polar stratospheric cloud of January 24, 1989, *Geophys. Res. Lett.*, **17**, 413-416.
- Dye J. E., D. Baumgardner, B. W. Gandrud, S. R. Kawa, K. K. Kelly, M. Loewenstein, G. V. Ferry, K. R. Chan, and B. L. Gary (1992) Particle size distribution in Arctic polar stratospheric clouds, growth and freezing of sulfuric acid droplets, and implications for cloud formation, *J. Geophys. Res.*, **97D**, 8015-8034.
- Dye, J. E., et al. (1996) In-situ observations of an Antarctic polar stratospheric cloud during ASHOE/MAESA: Similarities with Arctic observations, *Geophys. Res. Lett.*, **23**, 1913-1916.
- Fahey, D. W., K. K. Kelly, G. V. Ferry, J. R. Poole, J. C. Wilson, D. M. Murphy, M. Loewenstein, and K. R. Chan (1989) In Situ measurements of total reactive nitrogen, total water, and aerosol in a polar stratospheric cloud in the Antarctic, *J. Geophys. Res.*, **94**, 11,299 - 11,316.
- Farman, J. C., B. G. Gardiner, J. D. Shanklin (1985) Large losses of total ozone in Antarctica reveal seasonal ClO<sub>x</sub>/NO<sub>x</sub> interaction, *Nature*, **315**, 207-201.
- Hanson D. R. and K. Mauersberger (1988) Laboratory studies of the nitric acid trihydrate: implication for the south polar stratosphere, *Geophys. Res. Lett.*, **15**, 855-858.
- Hofmann, D. J., T. Deshler, F. Arnold, and H. Schlager (1990) Balloon observations of nitric acid aerosol formation in the Arctic stratosphere: II aerosol, *Geophys. Res. Lett.*, **17**, 1279-1282.
- Hofmann, D. J. and T. Deshler (1991) Stratospheric cloud observations during formation of the Antarctic ozone hole in 1989, *J. Geophys. Res.*, **96**, 2897-2912.
- Jäger, H., O. Uchino, T. Nagai, T. Fujimoto, V. Freudenthaler, and F. Homburg (1996) Ground-based remote sensing of the decay of the Pinatubo eruption cloud at three northern hemisphere sites, *Geophys. Res. Lett.*, **22**, 607-610.
- Kawa, S. R., D. W. Fahey, K. K. Kelly, J. E. Dye, D. Baumgardner, B. W. Gandrud, M. Loewenstein, G. V. Ferry, and K. R. Chan (1992) The Arctic polar stratospheric cloud aerosol: Aircraft measurements of reactive nitrogen, total water, and particles, *J. Geophys. Res.*, **97**, 1925 - 1938.
- Marti J., and K. Mauersberger (1993) Laboratory simulations of PSC particle formation, *Geophys. Res. Lett.*, **20**, 359-362.
- Molina M. J., R. Zhang, P. J. Wooldridge, J. R. McMahon, J. E. Kim, H. J. Chang, K. B. Beyer (1993) Physical chemistry of the H<sub>2</sub>SO<sub>4</sub>/HNO<sub>3</sub>/H<sub>2</sub>O system: implications for polar stratospheric clouds, *Science*, **261**, 1418-1423.
- Murcray, F. J., J. R. Starkey, W. J. Williams, W. A. Matthews, U. Schmidt, P. Amedieu, and C. Camy-Peyret (1994) HNO<sub>3</sub> profiles obtained during the EASOE campaign, *Geophys. Res. Lett.*, **21**, 1223-1226.
- Oelhaf, H., T. v. Clarmann, H. Fischer, F. Friedl-Vallon, Ch. Fritzsche, A. Linden, Ch. Piesch, M. Seefeldner, and W. Völker (1994) Stratospheric ClONO<sub>2</sub> and HNO<sub>3</sub> profiles inside the Arctic vortex from MIPAS-B limb emission spectra obtained during EASOE, *Geophys. Res. Lett.*, **21**, 1263-1266.
- Ovarlez, J. and H. Ovarlez (1994) Stratospheric water vapor content evolution during EASOE, *Geophys. Res. Lett.*, **21**, 1235-1238.
- Pueschel R. F., K. G. Snetsinger, J. K. Goodman, O. B. Toon, G. V. Ferry, V. R. Overbeck, J. M. Livingston, S. Verna, W. Fong, W. L. Starr, and R. K. Chan (1989) Condensed nitrate, sulfate, and chloride in Antarctic stratospheric aerosols *J. Geophys. Res.*, **94**, 11271-11284.
- Rosen, J. M. (1964) The vertical distribution of dust to 30 km, *J. Geophys. Res.*, **69**, 4673-4676.

- Rosen, J. M., S. J. Oltmans, and W. F. Evans (1989) Balloon-borne observations of PSCs, frost point, ozone, and nitric acid in the north polar vortex, *Geophys. Res. Lett.*, *16*, 791 - 794.
- Santee, M. L., G. L. Manney, W. G. Read, L. Froidevaux, and J. W. Waters (1996) Polar vortex conditions during the 1995-1996 Arctic winter: MLS ClO and HNO<sub>3</sub>, *Geophys. Res. Lett.*, *23*, 3203-3206.
- Schlager, H., F. Arnold, D. Hofmann, and T. Deshler (1990) Balloon observations of nitric acid aerosol formation in the Arctic stratosphere: I. Gaseous nitric acid, *Geophys. Res. Lett.*, *17*, 1275-1278.
- Schoeberl, M. R., L. R. Lait, P. A. Newman, and J. E. Rosenfield (1992) The structure of the polar vortex, *J. Geophys. Res.*, *97*, 7859-7882.
- Solomon S. (1990) Progress towards a quantitative understanding of Antarctic ozone depletion, *Nature*, *347*, 347-354.
- Spreng, S., and F. Arnold (1994) Balloon-borne mass spectrometer measurements of HNO<sub>3</sub> and HCN in the winter Arctic stratosphere - Evidence for HNO<sub>3</sub> processing by aerosols, *Geophys. Res. Lett.*, *21*, 1251-1254.
- Steele H. M. and P. Hamill (1981) Effect of temperature and humidity on the growth and optical properties of sulfuric acid-water droplets in the Stratosphere, *J. Aerosol Sci.*, *12*, 517-528.
- Tabazadeh, A., R. P. Turco, K. Drdla, and M. Z. Jacobson (1994) A study of type I polar stratospheric cloud formation, *Geophys. Res. Lett.*, *21*, 1619-1622.
- Thomason, L. W., L. R. Poole, and T. Deshler (1997) Global climatology of stratospheric aerosol surface area density deduced from stratospheric aerosol and gas experiment II measurements, *J. Geophys. Res.*, in press.
- Toon O. B., P. Hamill, R. P. Turco, and J. Pinto (1986) Condensation of HNO<sub>3</sub> and HCl in the winter polar stratospheres, *Geophys. Res. Lett.*, *13*, 1284-1287.
- Vömel, H., S. J. Oltmans, D. J. Hofmann, T. Deshler, and J. M. Rosen (1995) The evolution of the dehydration in the Antarctic stratospheric vortex, *J. Geophys. Res.*, *100*, 13919-13926.
- Worsnop, D. R., L. E. Fox, M. S. Zahniser, S. C. Wofsy (1993) Vapor pressures of solid hydrates of nitric acid: Implications for polar stratospheric clouds, *Science*, *259*, 71-74.
- Zhang, R., P. J. Woolridge, and M. J. Molina (1993) Vapor pressure measurements for the H<sub>2</sub>SO<sub>4</sub>/HNO<sub>3</sub>/H<sub>2</sub>O and H<sub>2</sub>SO<sub>4</sub>/HCl/H<sub>2</sub>O systems: Incorporation of stratospheric acids into background sulfate aerosols, *J. Phys. Chem.*, *97*, 8541-8548.